Lifecycle Cost Comparisons for Different Structural Systems Designed for the Same Location

V. Terzic, S.K. Merrifield & S.A. Mahin
Pacific Earthquake Engineering Research Center (PEER), University of California, Berkeley

SUMMARY:
Recent earthquakes in Chile, New Zealand and Japan revealed that modern buildings were generally safe. Still, there was tremendous variation in consequences associated with damage repair and loss of occupancy. This could be avoided by mitigating seismic damage through structural design. Although structural enhancements would likely increase the initial cost, it is expected that this might be compensated by benefits realized over the life of a facility. Thus, the selection of a structural system in an earthquake prone region should be based on the lifecycle cost rather than the initial cost. This paper presents the results of lifecycle cost analyses of three different structural systems designed for the same location. The buildings are representative of widely used, low-rise steel commercial buildings. They are located at a site having high seismic hazard representative of western North America. The analysis reveals significantly smaller lifecycle cost of systems with the improved seismic performance.

Keywords: steel, isolated building, PACT, PBEE methodology, non-structural damage

1. INTRODUCTION

Structures are generally designed to achieve functional requirements with adequate safety and minimum costs. However, when severe ground shaking occurs, damage to nonstructural components and the structural system can result in loss of function during extensive repairs. Such disruptions have a dramatic impact on the occupants, owners and community. Often, these situations can be avoided by mitigating seismic damage by means of improved structural design. Although structural enhancements would likely increase the initial structural cost, it is expected that this would be compensated by benefits realized over the life of a facility. Thus, choice of a structural system in the earthquake prone region should ideally be governed by the lifecycle cost rather than by the initial cost.

Performance-based earthquake evaluation (PBEE) is a powerful tool for assessing the likely performance of structures over their operational life or to scenario events. Fundamentally, performance is expressed in terms of variables of concern to stakeholders having on-going interests in the facility; i.e., owners, occupants and public officials as well as representatives of financial and insurance companies. As such, seismic performance is most often expressed in terms of direct costs of construction and repair, impacts associated with loss of use, and the potential for injuries and casualties. Given the uncertainty regarding the characteristics of future earthquakes and seismic response, performance is generally described in probabilistic terms. For instance, the mean annual expected costs associated with seismic repairs, and the confidence that downtime will not exceed a specified value (i.e., 72 hours).

Methodologies to systematically characterize earthquake hazards and risks have been extensively developed. One such method was developed by the Pacific Earthquake Engineering Research Center (PEER), and further refined by ATC (2012a). The computational tool, PACT has been developed as part of that effort to estimate repair costs and times needed to implement repairs. Little information is

available on downtime associated with planning and on impacts associated with loss of function.

In this paper, PBEE methods are used to evaluate the relative performance of a three-story office building located at a site having high seismic hazard representative of western North America. Three alternative lateral load-resisting systems are considered. A special moment resisting frame (SMRF) designed to code minimums was selected as the baseline case. It was designed with a force reduction factor (R) of 8 utilizing reduced beam sections (prequalified beam-to-column connection). As an alternative, a base-isolated intermediate moment resisting frame (BI-IMRF) was chosen. It was also designed to meet minimum code requirements (R=2), but has simpler connection details and does not require a strong column-weak girder design approach. Taking this a step further, an isolated system with superstructure designed to remain elastic (R=1) was considered as the final alternative.

Lifecycle cost analysis is performed considering three hazard levels: 50%/50 years (SLE), 10%/50 years (DBE), and 2%/50 years (MCE). It is based on the initial cost, expected repair cost, and the minimum monetary loss due to business interruption following an earthquake. In addition, comparisons are made considering structural responses (such as median values of maximum story drift and maximum floor acceleration) and repair costs for each hazard level. Emphasis is placed on those factors that contribute significantly to the economic losses, the ability of various structural systems to reduce these losses, and the adequacy of current methods for estimating decision variables (DV).

2. BUILDINGS CONSIDERED

A three-story tall, steel office building is considered for all of the cases. The basic building plan dimensions are 36.6 m (120 ft) by 54.9 m (180 ft), with a typical bay spacing of 9.14 m (30 ft) in each direction. Story heights for all systems are 4.57 m (15 ft), except for the first story of the SMRF system, which is 5.18 m (17 ft). The systems adhering to the code minimum (SMRF and BI-IMRF with R=2) were designed by a professional engineering firm (Morgan, 2008) utilizing the Equivalent Lateral Force Method (ASCE -7, 2005). The BI-IMRF designed with R=1 was designed by the authors of this paper, and the elevation is shown in Figure 1. The buildings were assumed to be located on stiff soil (site class D with reference shear wave velocity = 180 to 360 m/s). Code spectral accelerations were selected to be Ss = 2.2g for short periods and S1 = 0.74g at a period of 1 sec, which are representative of many locations in California.

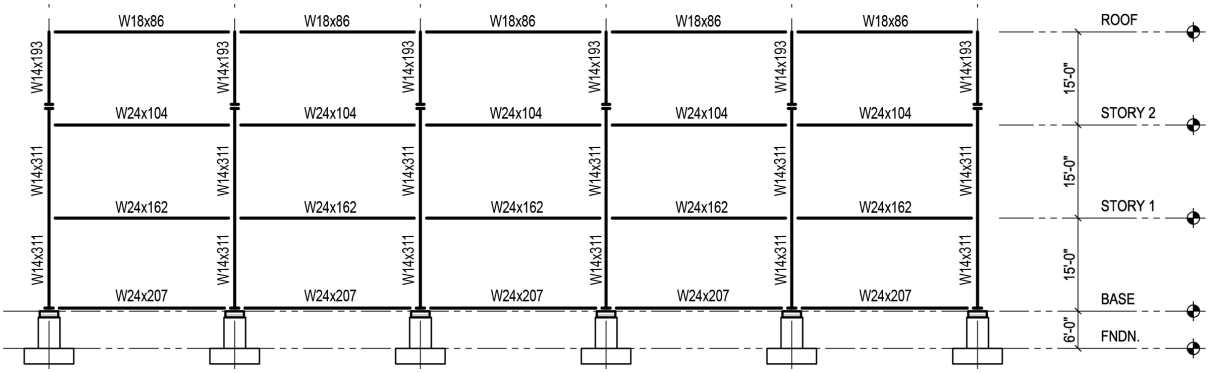

Figure 1. Isolated IMRF designed utilizing the R factor of 1

3. GROUND MOTIONS

The set of ground motions used in the analysis were selected to match the uniform hazard spectrum and associated causal events for a site in Oakland, California. Forty 3-component ground motion records were selected to represent the ground motion hazard at each of three hazard levels (2%, 10% and 50% probabilities of exceedence in 50 years). More information on these motions can be found

elsewhere (Baker, 2010). Figure 2 shows good agreement between the median pseudo-acceleration response spectra for the fault parallel (FP) and fault normal (FN) components of the 10% in 50-year and 2% in 50-year hazard level events and the code stipulated DBE and MCE spectra used in the design of the buildings.

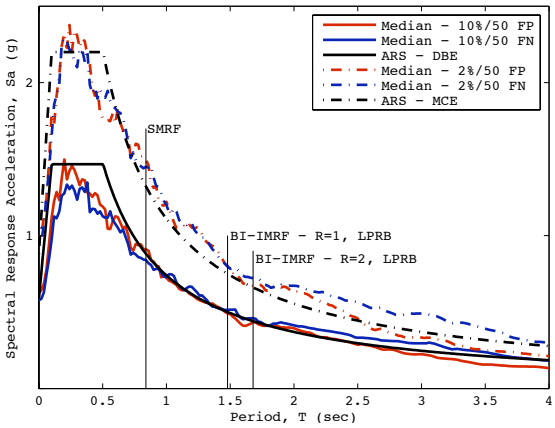

Figure 2. Comparison of code stipulated DBE and MCE spectra with the median pseudo-accelerations for fault normal (FN) and fault parallel (FP) components of the 10% in 50-year and 2% in 50-year hazard level events used in analysis

4. ANALYSIS MODEL AND METHODS

To simplify the analysis for the purpose of this comparison, the time history analyses of all buildings are performed on appropriately modeled 2D frames. The lateral load resisting frames described above were used only on the perimeter of the building. Gravity-load-only type connections were used elsewhere in the structure. Additional modeling assumptions are described below:

1. Half of the lateral floor mass was assigned at each floor of the 2D frame, equally distributed among all nodes of that floor. Vertical mass equal to the (tributary weight)/g was assigned to the same nodes.
2. Floor slabs were assumed to be axially inextensible.
3. P-Δ effects from the gravity columns are accounted for by using leaning column (Gupta and Krawinkler, 1999). The gravity load was equal to the half of the gravity load per floor minus gravity load acting on the columns of the lateral load-resisting frame. The leaning column was modeled with concentrated plastic hinges at the element ends (one column per story). The moment capacity of the plastic hinges was equal to the summation of the capacities of all the other columns that were not part of laterally resisting system under consideration divided by 2. The leaning column was constrained to have the same lateral displacement as lateral load-resisting frame.
4. The effects of large deformations of beam and column elements are accounted for utilizing P-Δ nonlinear geometric transformation.
5. The frames were subjected to either FP or FN components of ground motion in combination with the vertical component.

The numerical model was implemented in OpenSees (McKenna and Fenves, 2004). Centerline models were used for both structural systems, SMRF and BI-IMRFs. Beams of the SMRF utilized the reduced beam section (RBS) and were thus modeled with elastic elements and concentrated plastic hinges. The elastic portion of the element was modeled with modified stiffness so that the equivalent stiffness of rotational spring - elastic element - rotational spring assembly is equivalent to the stiffness of the actual frame member (Ibarra and Krawinkler, 2005). Hinges are defined with zero-length elements (rotational springs). The hinge moment-rotation relationship was defined using Hysteretic Material of OpenSees. The moment-rotation relationships for RBS connections are developed based on recommendations from PEER/ATC (2010), and calibrated to closely resemble experimental results for RBS connections performed by Uang (2000). Columns of the SMRF, as well as beams and columns of IMRFs are modeled utilizing two element types. Panel zone regions are modeled with elastic elements.

The portion of beams and columns along the clear element length is modeled utilizing force-based beam-column elements (FB-BCE) of OpenSees (with fiber section), which considers distribution of plasticity along the element. The Menegotto-Pinto hysteretic model is used for the steel fibers. Fatigue of beams and columns was accounted for by using well-calibrated fatigue model for I-sections (Uriz and Mahin, 2008). The number of integration points along the FB-BCE length is selected such that the integration weights at the locations of plastic hinges match the plastic hinge length, assumed to be (2/3) of the element depth.

For the isolated systems, isolators are modeled with zero-length elements (horizontal springs), one beneath each column of the structural frame. Vertical displacements and rotations at the top and the bottom of isolators were assumed to be fixed. The leaning column has a roller in the horizontal direction at its base, so it can follow displacements of the structural frame. To represent hysteretic behavior of bearings, bi-linear and tri-linear models are used for the LPRBs and TFPBs, respectively. The model of the LPRB was designed to meet the characteristics of the seismic isolation system set by the designer (Morgan, 2008). In the MCE case, the effective period, the effective damping, and maximum horizontal displacement were T_{eff} = 3.07 sec, β_{eff} = 15.8%, and D_M = 61.7 cm. For DBE, these parameters were T_{eff} = 2.77 sec, β_{eff} = 24.2%, and D_D = 32.3 cm. The model of the TFPB was designed to meet characteristics of the seismic isolation system for the DBE level. Hysteretic behavior of the two bearing types is given in Figure 3.

Damping was assigned to the frames based on PEER/ATC (2010) recommendations. The damping ratio was taken to be 3% for both structural systems. For the fixed-base building, mass and tangent stiffness proportional Rayleigh coefficients were calculated based on two periods. The first (T_1) and third (T_3) periods were selected for the 50% in 50-year hazard level, and $1.5T_1$ and T_3 for the DBE and MCE events. The first period is elongated 1.5 times to account for the change in period due to the nonlinear deformations of the system. For the isolated building the damping was proportional to the tangent stiffness of the structure. The stiffness-proportional damping is calculated from the fundamental period of the structure T_1 for the 50% in 50-year hazard, and T_{eff} for the DBE and MCE hazards, where T_{eff} is the effective fundamental period of the seismically isolated structure. As stated in the previous paragraph, T_{eff} is different at each hazard level. Stiffness proportional damping of the two structural systems is applied only to the frame elements and not to the: (i) elements of the leaning column, (ii) highly rigid truss elements that link the frame and leaning column, and (iii) zero-length elements that were used to model beam plastic hinges of SMRF and bearings of BI-IMRF. The stiffness of the elastic beam elements of SMRF was modified, and thus the stiffness proportional damping coefficients used with these elements were also modified as suggested by Zareian and Medina (2010).

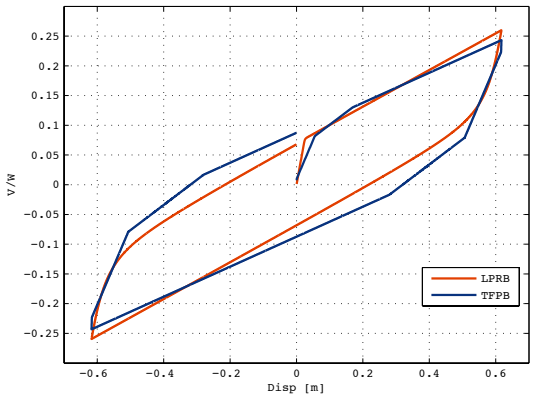

Figure 3. Hysteretic behaviour (normalized force vs. displacement) at MCE level of lead-plug rubber bearing (LPRB) and triple friction pendulum bearing (TFPB)

5. COMPARISON OF RESPONSE

While numerous parameters need to be considered to fully evaluate structural response, it is common

to correlate performance to engineering demand parameters based on peak story drift, peak floor level accelerations and residual drifts. The median peak story drifts and floor accelerations for the 50%, 10% and 2% probabilities of exceedence in 50 years are shown in Figures 4 and 5, respectively. Results for residual displacements are not shown in these comparisons. The plots show the median of the average response from the FN and FP component of the ground motion.

At the 50%/50-year hazard level, Figure 4(a) shows that the BI-IMRF with R=1 is the most effective in limiting story drifts. It is notable that the median story drifts for the BI-IMRF with R=2 are slightly higher at the second and the third story compared to the fixed-base SMRF. This is attributed to the greater flexibility of the isolated moment frame that utilizes the R factor of 2. Compared to the fixed-based frame, the substantial reduction in base shear for the isolated moment frame results in disproportionately smaller members, and thus a more flexible system with larger drifts. The type of bearing does not have significant influence on the median story drifts for this hazard level. All three frames are expected to yield at drifts slightly larger than 1%, so elastic behavior is expected at this level of excitation. However, the damage of interior partitions and stairs will be initiated for SMRF and BI-IMRF R=2 systems, as the median triggers for damage of stairs and partitions (0.5% and 0.64%, respectively) are lower than the peak median drifts of these two systems (0.77% and 0.7%, respectively).

At the design level (10%/50-year) excitation, Figure 4(b) greater differences in story drifts are observed among the three systems. The BI-IMRF with R=1 is again the most effective in limiting story drifts. There is about a 40% reduction compared to the R=2 system, and about 60% compared to the SMRF system. For this system, peak median story drifts for both bearing types are around 0.7%, which is not large enough to induce structural damage, but may initiate damage of the interior partitions and stairs. Peak median story drifts for the BI-IMRF R=2 system are higher at around 1.1% for both bearing types, which again suggest structural damage will be avoided, but probable damage to non-structural partitions and stairs. The fixed base SMRF has the largest drifts among all of the systems at every level, with peak median value reaching 1.63%. Although the yielding of the system is initiated, significant repair of the structural components is not expected. However, more significant repairs of interior partitions, exterior cladding, and stairs are expected on SMRF relative to BI-IMRFs.

At the MCE hazard (2%/50-year) level, Figure 4(c) shows even greater differences in story drifts among the three systems. At this hazard level the advantage of using TFPBs becomes apparent for the BI-IMRF R=2 system. This is attributed to larger isolator displacements, in which hysteretic behavior of the two isolator types start to diverge. Again, the BI-IMRF with R=1 has the smallest median story drifts among the three systems, and compared to BI-IMRF R=2 and SMRF, reductions are ~50% and ~70%, respectively. For this system the peak median story drift is ~0.9% for both bearing types. Although structural damage is not expected at these drift levels, damage to interior partitions and stairs will initiate. For the BI-IMRF with R=2 system, the peak median story drift is 1.7% when the LBRB is used and 1.47% when the TFPB is used. Although structural damage of IMRF panel zones may be anticipated at these drift levels, this was not considered in the loss study due to lack of repair cost information. The fixed base SMRF has the highest peak median drift of 2.8%. This drift is within the expected capacity of prequalified RBS connections, but will likely necessitate significant repairs throughout the structure.

Two things are immediately apparent from the floor acceleration demands (Figure 5). First, BI-IMRFs with R=1 and 2, irrespective of bearing type, result in similar acceleration demands. In addition, the isolated systems achieve substantial reduction in floor accelerations compared to the fixed-base SMRF. For the three hazard levels the reduction in peak median total acceleration in the range of 61-73%. The peak median total accelerations of isolated systems at the three considered hazard levels range from 0.23g to 0.4g. At these accelerations, significant damage to contents and non-structural components are not expected. For the fixed base SMRF, the peak median total accelerations range from 0.6g-1.33g. At the 50%/50-year hazard level, the median acceleration in the range from 0.25g to 0.6g over the height of the building will trigger damage of roof tiling, chillers, suspended ceilings and office components. The design level (10%/50-year) excitation, with the median acceleration in the

range from 0.5g to 1.15g over the height of the building, will additionally trigger the damage of HVAC and cooling tower. The same type of damage is expected for the MCE hazard (2%/50-year) level but to the greater extent.

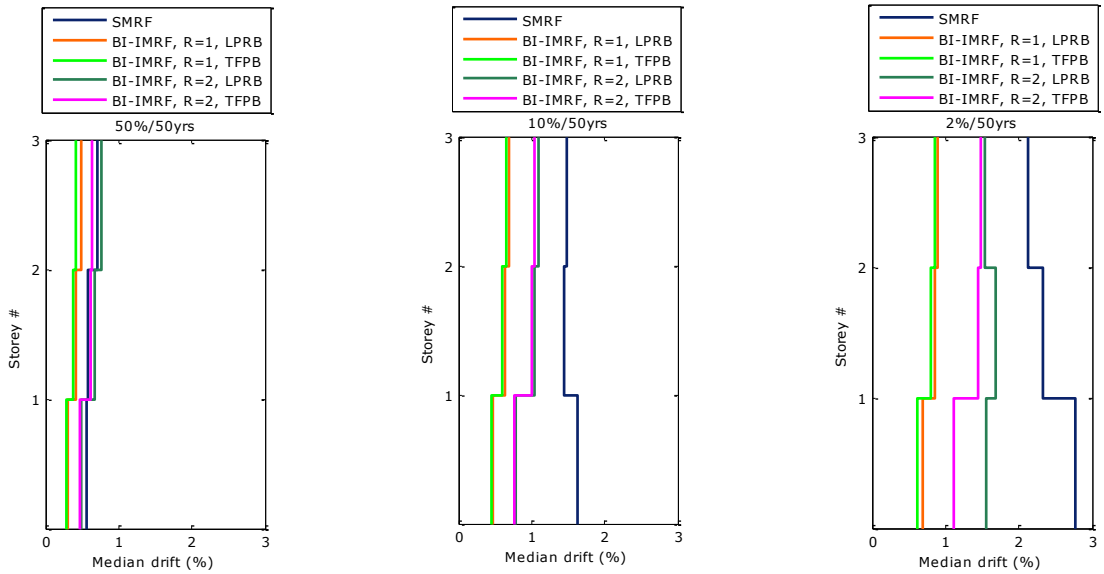

Figure 4. Median drift of the SMRF and the BI-IMRFs for three hazard levels (a) 50%/50yrs., (b) 10%/50yrs., (c) 2%/50yrs. Results include response of BI-IMRFs considering two different framing designs (R=1, and R=2) and two different isolator types (LPRB and TFPB).

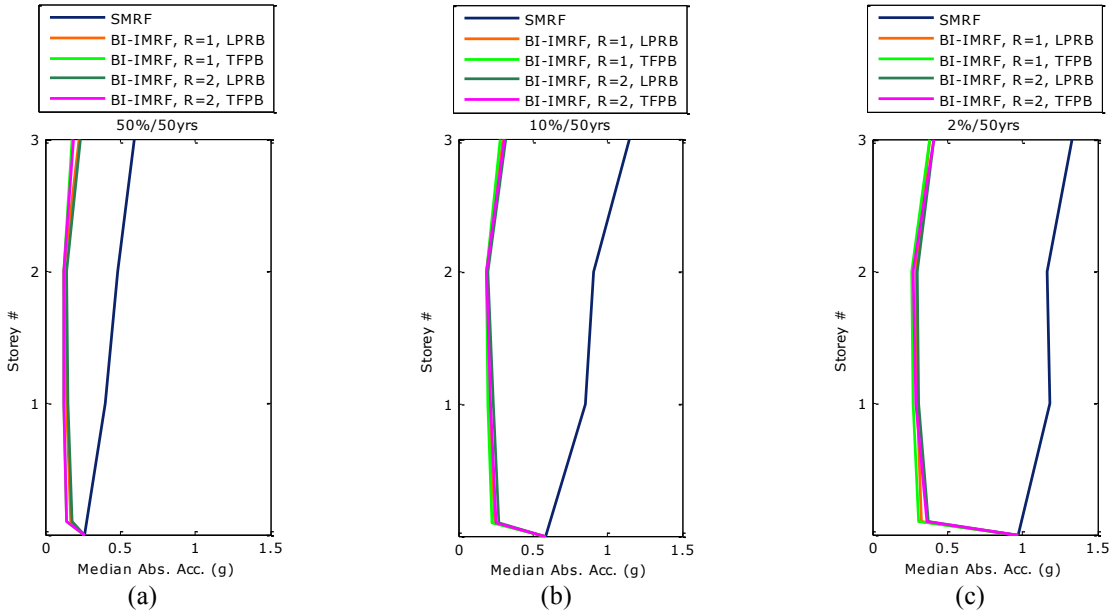

Figure 5. Median acceleration of the SMRF and the BI-IMRFs for three hazard levels (a) 50%/50yrs., (b) 10%/50yrs., (c) 2%/50yrs. Results include response of BI-IMRFs considering two different framing designs (R=1, and R=2) and two different isolator types (LPRB and TFPB).

It is clear that isolation substantially reduces the accelerations. The reduction in drift is also apparent, especially for the IMRF design that utilized the R factor of 1. In addition to preserving the elastic behavior of the structure at all hazard levels this system also minimizes nonstructural damage. Triple friction pendulum bearings provide slightly better structural response than the lead-plug rubber bearings used. However, refinement of the bearing models is necessary to confirm this advantage of

one bearing type over the other.

6. PERFORMANCE ASSESSMENT

The effectiveness of an isolated system was assessed by comparing the savings in repair and business interruption cost relative to the added initial cost. This was done using the computer software Performance Assessment Calculation Tool (PACT II). Two types of assessments were performed: intensity-based and time-based assessments. In the intensity-based assessment two DVs, repair costs and business downtime, were determined for every system at each hazard level. For the time-based assessments, the DVs for each hazard are weighted according to the probability of occurrence for each hazard and then integrated to determine a total life cycle loss, expressed in an equivalent annualized value.

Table 1 summarizes the initial building costs for each system considered in this study. Building content was assumed to be consistent throughout all systems, and a metric of \$250/sq ft (\$2690/m^2) was used to estimate the total fixed-base building cost, in which the structural costs accounts for around 12% of the cost. For the isolated systems a metric of \$50/sq ft (\$538/m^2) was added to the fixed-base cost, but savings from smaller structural members and less stringent detailing for IMRF systems were also considered. BI-IMRF R=2 and 1 designs were expected to save 25% and 10% in structural costs, respectively. These estimates are preliminary, and will be refined in future phases of this study. Although two types of isolators, LPRB and TFPB, were implemented in this study, the relative differences in their costs were not considered and will be left for future study as well.

Table 1. Initial costs expressed in 1000 USD

	SMRF	BI-IMRF R = 2	BI-IMRF R = 1
Material Savings	-	-500	-200
Isolation Cost	-	1,080	1,080
Net Increase	-	580	880
Total Building Cost	**16,200**	**16,780**	**17,080**

In order to determine the repair and business interruption costs, the EDPs obtained from the OpenSees model had to be converted to these DVs using PACT II. The PACT II modeling process is essentially broken down into three stages. The user first describes the basic building information, such as its replacement cost, occupancy type, footprint, and story height. The user proceeds to define the building's structural system and non-structural content, including the expected quantities for each component. The type and quantities of most non-structural content were determined using the normative quantities recommended by ATC-58 (ATC, 2012). In the final stage of the modeling process, the EDPs are specified for each scaled ground motion within each earthquake hazard level. In order to perform life-cycle assessments, each hazard level's mean annual frequency of exceedence (MAFE) was specified as well. Once the model is prepared, PACT II performs simulations using the Monte Carlo method, generating a large number of possible outcomes and the associated DVs for each component. Total losses are then computed using simple Euler integration.

Table 2 displays the relative savings compared to the SMRF system, expressed in both absolute and percentage figures. It indicates that in DBE and MCE hazards, all isolated systems have median repair cost savings that far outweigh the added isolation costs. Even for the frequent service hazard level, expected savings from improved performance are close to or greater than the added initial costs. TFPB isolators perform better than LPRB isolators, with the greatest savings achieved when TFPB isolators are used in combination with a superstructure designed to remain elastic at the DBE level. The benefit of a structure designed with an R factor of 1 becomes more pronounced at the MCE level, since the structure designed with an R factor of 2 experiences large story drifts that cause significant damage to the structure, exterior cladding, and interior partitions. Without even considering added costs due to business interruption, the intensity-based assessment indicates that isolated systems significantly reduce costs for all hazard levels.

Table 2. SMRF baseline construction repair cost savings in 1000 USD

HL	CL	Measure	BI-IMRF			
			LPRB		TFPB	
			R = 2	R = 1	R = 2	R = 1
50% - 50yr	50%	$ Sav.	484	856	643	929
		% Red.	47%	83%	62%	90%
	90%	$ Sav.	809	1,438	1,038	1,611
		% Red.	43%	76%	55%	85%
10% - 50yr	50%	$ Sav.	2,336	3,233	2,468	3,312
		% Red.	62%	86%	65%	88%
	90%	$ Sav.	2,288	4,587	2,991	4,729
		% Red.	40%	79%	52%	82%
2% - 50yr	50%	$ Sav.	1,168	4,936	2,523	5,359
		% Red.	18%	74%	38%	81%
	90%	$ Sav.	190	4,082	756	6,990
		% Red.	2%	39%	7%	67%

PACT II also provides downtime estimates, but with limited accuracy. Building downtime is influenced by numerous factors, and difficult to accurately estimate at higher hazard levels. Service level hazards are expected to cause minimal damage, so the downtime would approximately be equivalent to the construction repair time, but for higher hazard levels which are expected to cause extensive damage, added factors such as financing, relocation of operations, manpower availability, and economic uncertainty can amount to delays on the order of years (Comerio, 2005). Unlike construction repair estimates, these added factors are difficult to quantify, since they would vary significantly case by case.

For the purposes of this study, construction repair times estimated by PACT were only considered, as this would indicate a lower bound on the downtime estimates. In determining this lower bound, PACT assumes all construction repair takes place simultaneously on all floors, but for each floor it also assumes components are repaired sequentially. In reality, multiple components on a floor would be undergoing simultaneous repair, and therefore lower construction downtime estimates may be achieved. However, irrational downtime factors are not considered, so downtime estimates should still remain conservative. These downtime estimates are shown on Table 3. Similar to repair costs, the benefit of designing a superstructure with an R factor of 1 is obvious.

Table 3. Construction repair time estimates expressed in days

HL	CL	SMRF	BI-IMRF			
			LPRB		TFPB	
			R = 2	R = 1	R = 2	R = 1
50% - 50yr	50%	24	16	5	11	2
	90%	48	36	15	26	8
10% - 50yr	50%	92	40	14	36	12
	90%	151	91	33	77	29
2% - 50yr	50%	175	139	44	109	31
	90%	273	244	155	229	88

It is beneficial to convert the business downtime estimates to equivalent business interruption costs, such that they can be added with the repair costs to determine a total cost at each hazard level. To do this, a metric that converts downtime to an equivalent interruption cost was estimated. Similar to downtime estimates, irrational factors that may affect profit were not considered, and it is also assumed that the entire building is inoperable during downtime. If the owner were leasing the building property to businesses, then the downtime losses would be equivalent to the loss in income from leasing space. If the owner were a business headquartered in the facility with no other branches to

relocate to, the downtime losses would be the cost of leasing and relocating to a different space. It was assumed that all 3-story buildings with similar footprints in downtown Oakland would charge the same rent, and was estimated to a metric of $20/sq ft/year (LoopNet, 2012). This is equivalent to a business interruption cost of $3550/day.

Table 4 expresses the total repair cost of every system at each hazard level. All losses are expressed in thousands of USD. The contribution of losses due to business downtime to the total loss remains fairly constant at 7-9% for every hazard level and every system type. Again, business downtime contributions represent a lower bound, and for higher hazard levels larger losses due to downtime should be expected.

Table 4. Intensity-based total loss in 1000 USD

HL	CL	SMRF	BI-IMRF			
			LPRB		TFPB	
			R = 2	R = 1	R = 2	R = 1
50% -50yr	50%	1,115	603	192	426	108
	90%	2,073	1,222	518	957	320
10% - 50yr	50%	4,107	1,586	597	1,440	511
	90%	6,324	3,823	1,318	3,070	1,162
2% - 50yr	50%	7,270	5,970	1,860	4,510	1,400
	90%	11,340	11,050	6,840	10,430	3,690

Time-based assessments recognize the time-value of money. It allows owners to assess the effectiveness of isolation through a cash flow analysis. Construction cost inflation and desired discount rates cause the relative savings realized in isolated systems to diminish over time. To simplify the cash flow analysis, it is assumed that discount rates are adjusted to incorporate the expected average inflation rate in a 50 year time period. According to Figure 7, the average US inflation rate in the past century has been at around 3% (Capitol Professional Services, 2011).

Similar to the intensity-based total losses, annual downtime estimates were converted into equivalent business interruption losses, using the same metric of $3550/day. Eqn. 6.1 was used to determine the net present value (NPV) of each isolated system relative to the SMRF system:

$$NPV = \frac{1-(1+i)^{-n}}{i} A_{sav} - P_i \tag{6.1}$$

where i is the discount rate, n is the building life-cycle, A_{sav} is the total annual savings of the isolation system with respect to the SMRF, and P_i is the added initial cost of the isolation system.

Table 5 displays the median annualized total loss for each structural system, as well as the maximum discount rate that can be obtained before losing the benefit of using an isolated system (i.e., discount rate at which NPV = 0). It is evident that the BI-IMRF with R=1 using TFPBs would provide the most life-cycle savings for the situation considered in this study. All isolation systems provide life-cycle benefits that outweigh the added cost of using isolators, even if an average inflation rate of 3% is assumed. For all systems, greater savings are expected if downtime estimates are further refined.

Table 5. Time-based results showing median annualized total loss in USD and maximum discount rates relative to the SMRF system.

	SMRF	BI-IMRF			
		LPRB		TFPB	
		R = 2	R = 1	R = 2	R = 1
Median Annualized Total Loss (USD)	56,240	31,930	12,330	26,290	8,966
Max. Discount Rate	-	3.4%	4.4%	4.7%	4.9%

CONCLUSION

Performance-based earthquake evaluation has developed over the past two decades to a point where it can be applied to particular structures. In design, it can be used to identify systems, proportions and details that can improve the overall performance of structures considering minimization lifecycle losses associated with casualties, repair and downtime. However, more work is needed to develop and validate specific quantitative information on the losses and consequences of damage to the structural system, nonstructural elements and contents.

As shown in this study, isolated systems provide significant damage savings at all three hazard levels, justifying the initial added cost. Furthermore, improvements of the isolation system beyond code minimum standards resulted in not only superior performance, but a significant reduction in lifecycle cost as well. This is attributed to the orientation of current US Codes towards a focus on preventing collapse rather than minimizing economic loss. Thus, current codes may be adequate for protection of life in most cases, but PBEE methodologies are needed to assess the ability of alternative and enhanced designs to achieve continued functionality of a structure following an earthquake and to achieve a desired return on the investment used to enhance performance.

AKCNOWLEDGEMENT
The authors acknowledge financial support for this work from the Pacific Earthquake Engineering Research Center. The authors are grateful for the Applied Technology Council providing a pre-release beta version of the PACT software application. The conclusions, observations and findings presented herein are those of the authors and not necessarily those of the sponsors.

REFERENCES

American Society of Civil Engineers. (2005). *Minimum Design Loads for Buildings and Other Structures*. ASCE, Reston, VA.

ATC. (2012a). *Development of Next Generation Performance-Based Seismic Design Procedures for New and Existing Buildings*. Applied Technology Council, Redwood City, CA. [electronic version: https://www.atcouncil.org/Projects/atc-58-project.html]

ATC. (2012b). *Performance Assessment Computation Tool (PACT-2)*. Applied Technology Council, Redwood City, CA. [electronic version: https://www.atcouncil.org/downloads/atc58installation.html]

Baker, J. W., Lin, T., Shahi, S. K., and Jayaram, N. (2011). *New ground motion selection procedures and selected motions for the PEER transportation research program*. Pacific Earthquake Engineering Research Center, University of California, Berkeley, CA, USA. Report PEER 2011/03.

Capitol Professoional Services. (2011). Average inflation rates by decade. *InflationData.com.* Retrieved April 25, 2012 from http://www.inflationdata.com/Inflation/Inflation/DecadeInflation.asp

Comerio, M. (2005). Estimating downtime in loss modeling. *Earthquake Spectra* **22:2**,349-365.

Gupta, A. and Krawinkler, H. (1999). *Seismic demands for performance evaluation of steel moment resisting frame structures*. Stanford University, Stanford, CA. Report No. 132 (p. 26-28).

LoopNet. (2012). 1212 Broadway. *LoopNet.com*. Retrieved April 25, 2012 from http://www.loopnet.com/xNet/MainSite/Listing/Profile/Profile.aspx?LID=16939663&SRID=2551381644&StepID=101

McKenna, F. and Fenves, G.L. (2004). *Open System for Earthquake Engineering Simulation (OpenSees)*. PEER, University of California, Berkeley, CA.

Morgan, T. (2008). *Structural Design Calculations and Drawings*. Forell/Elsesser Engineers, San Francisco.

PEER/ATC. (2010). *Modeling and acceptance criteria for seismic design and analysis of tall buildings*. PEER/ATC-72-1, prepared by the Applied Technology Council in cooperation with PEER, Redwood City, CA.

Uang, C. M. (2000). *Cyclic Response of RBS Moment Connections: Loading Sequence and Lateral Bracing Effects*. University of San Diego, San Diego, California. Report No. SSR-99/13.

Uriz, P., and Mahin, S. A. (2008). *Toward Earthquake-Resistant Design of Concentrically Braced Steel-Frame Structures*. Pacific Earthquake Engineering Research Center, University of California, Berkeley, CA, USA. Report PEER 2008/08.

Zareian, F. and Medina, R. A. (2010). A practical method for proper modeling of structural damping in inelastic plane structural systems. *Computers & Structures* **88:1-2**,45-53.